# DISCRETE PLY MODELLING OF LOW VELOCITY IMPACT AND COMPRESSION AFTER IMPACT IN UNIDIRECTIONAL LAMINATED COMPOSITES

C. Bouvet[1*], N. Hongkarnjanakul[1], S. Rivallant[1]

[1]*Université de Toulouse; INSA, UPS, Mines Albi, ISAE; ICA (Institut Clément Ader) – ISAE, 10 avenue Edouard Belin, 31055 Toulouse Cedex 4, France*
**christophe.bouvet@isae.fr*

**Keywords:** composite, impact damage, CAI, damage tolerance

## Abstract
*This paper deals with impact damage, permanent indentation and compression after impact (CAI) modelling. A model enabling the formation of damage developing during low velocity / low energy impact test and CAI test in laminated composite panels has been elaborated. The different impact and CAI damage types, i.e. matrix cracking, fibres failure and interfaces delamination, are simulated. This model is compared to experimental tests and is used to highlight the failure scenario of laminate during residual compression test. Finally the impact energy effect on the residual strength is evaluated and compared to experimental results.*

## 1. Introduction
Composite materials have been increasingly introduced in airframe and space applications in the last decades because of their interesting characteristics, like their low specific weight, enhanced mechanical strength, high stiffness... Nevertheless, during the structure's life, damage induced in these materials by impacts of minor and major objects, like hail stones, runway debris or dropping tools, can drastically decrease the structure's life.
Low velocity impact is one of the most critical loading for composite laminates. Indeed, for structures submitted to low energy impacts or minor objects drops, like tools during assembly or maintenance operations, composite laminates reveal a brittle behaviour and can undergo significant damage in terms of matrix cracks, fibres breakages or delaminations. This damage is particularly dangerous because it drastically reduces the residual mechanical characteristics of the structure, and at the same time can leave a very little visible mark onto the impacted surface [1].
Consequently, it is essential to define a damage tolerance demonstration to design this type of structure in order to take into account the possible damage. In the field of aeronautics, the damage tolerance, for damage corresponding to impact loading, drives to dimension the structure depending on the impact detectability [2]. If the damage is not detectable, in fact when the impact indentation is less than barely visible impact damage (BVID), the structure must support the extreme loads and if the damage is detectable, in fact when the impact indentation is bigger than BVID, another criterion must be considered, like repair or change of the structure [3, 4].
Then, in order to be able to numerically optimize a composite structure with impact damage tolerance concept, it is necessary to simulate, with the same model, the impact damage, and in particular the permanent indentation, and the CAI test to evaluate the residual strength versus impact energy and permanent indentation. This is the scope of the proposed model which is able to simulate the impact and the residual strength test.

In the literature, many authors have studied impact behaviour of composite structures and their effects on residual strength, both experimentally [1, 5, 6…], as well as numerically [1, 7, 8…], but a few works deal with numerical model taking into account impact and CAI modelling. The Faggiani and Falzon's [9] work should be noted, because it is, to our knowledge, the only model of literature used to simulate impact and compression after impact tests on a real structure. The numerical correlation seems to be good on time-force history, on damage shape and on residual strength. Nevertheless the insufficient knowledge of the real impact damage obtained experimentally induces difficult evaluation of the reliability of this model. In particular the ultrasonic investigations (C-Scan) given in this study do not allow to experimentally determine the delaminated interfaces shape and other experimental investigations, as micrographic cuts or following by image correlation during compression after impact test, should be necessary to evaluate the reliability of the model.
Here, this research paper is a complementary work from Bouvet et al. [10] who have developed an impact FE model, aiming to model impact damage and permanent indentation. This model is improved and is used to simulate the CAI test. In particular the fibres failure criterion under compression solicitation, which is of first importance during CAI test, has been modified. Finally this model is compared with experimental results of CAI tests with different impact energies. It allows to globally simulate impact damage, as delaminated area, fibres failure or permanent indentation, and the CAI damage, as fibres failure propagation or local buckling of delaminated zone.

## 2. Experimental study

Impact tests were performed in drop tower system (fig. 1a) with an impactor of 16 mm diameter and 2 kg, according to Airbus Industries Test Method (AITM 1-0010) [11]. The dimension of rectangular specimen is $100 \times 150 \times 4.16$ mm$^3$ simply supported to a boundary condition of $75 \times 125$ mm$^2$ window (fig. 1a). The laminated plate is manufactured with T700/M21 unidirectional carbon/epoxy composite of 0.26 mm ply thickness, with stacking sequence $[0_2, 45_2, 90_2, -45_2]_S$. Then CAI tests were performed on a hydraulic machine, the specimen being stabilized by a $90 \times 140$ mm$^2$ window (fig. 1b), according to Airbus Industries Test Method (AITM 1-0010) [11].

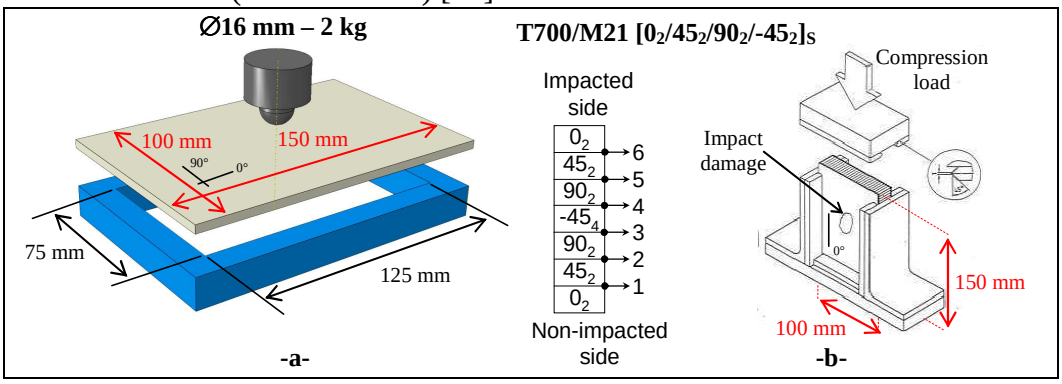


**Figure 1** (a) Impact test setup; (b) CAI test setup

## 3. Numerical Modelling

In previous study, Bouvet et al. [10] presented a discrete 3-dimensions model of impact with special mesh construction, oriented in 0°, 90°, 45° and -45° (fig. 2b). Positions of nodes are uniformly stacked in row and column for all ply orientations but the shapes of mesh are different: 0° and 90° plies are meshed in square shape, while 45° and -45° plies are meshed in parallelogram shape to follow the fibre direction. The model is simulated in explicit/dynamic response in Abaqus v6.9 with user subroutine Vumat. According to experimental observation,

impact damage can be separately modelled in (i) fibre failure, (ii) intra-ply matrix cracking and (iii) delamination in-between plies (fig. 2a).

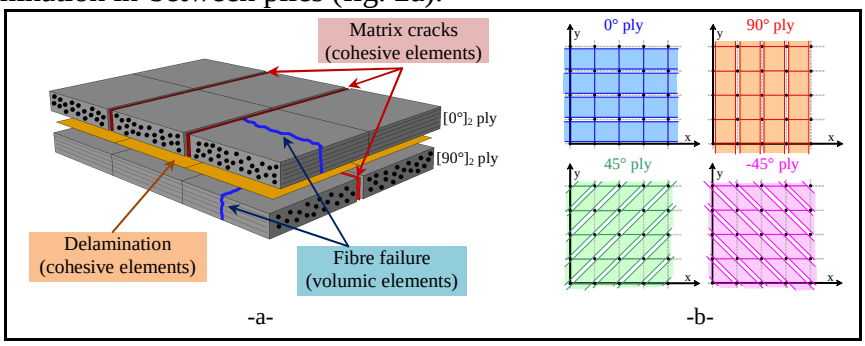


**Figure 2** Model of (a) impact damages and their element types; and (b) mesh shapes in each oriented ply

### *3.1 Modelling of fibre failure*

The fibres failure is taken into account using failure criterion written inside the volumic elements. This criterion is based on the fracture mechanics in order to be able to dissipate the critical energy release rate in opening mode (mode I) due to fibres fracture (fig 2a). In fact, the behaviour laws at the 8 Gauss points of a volumic element are driven together to dissipate the same energy as the critical energy release rate in mode I of a plane crack normal to the fibre direction through the element. Then for tension (fig. 3a), the material parameters (table 1) are the Young modulus $E_l^t$, the failure strain $\varepsilon_o^t$ and the critical energy release rate $G_I^t$. Of course, the classical elastic characteristics of the ply, $E_t$ the Young modulus in transverse direction, $\nu_{lt}$ the Poisson's ratio and $G_{lt}$ the shear modulus, are also needed. For compression (fig. 3a), a crushing plateau is added, and the material parameters are the Young modulus $E_l^c$, the failure strain $\varepsilon_o^c$, the critical energy release rate $G_I^c$ and the plateau stress $\sigma_0$. The energy release rate for compression is very difficult to evaluate and the meaning of this value is very complex [12] and seems to correspond to initiation value but not to propagation. In fact, for this modelling, the propagation value is needed and to overcome this problem, an artificially low value (table 1) was adopted in order to avoid this phenomenon dissipates too much energy. This point is currently studied and should be confirmed with other experimental tests inducing compression fibre failure.

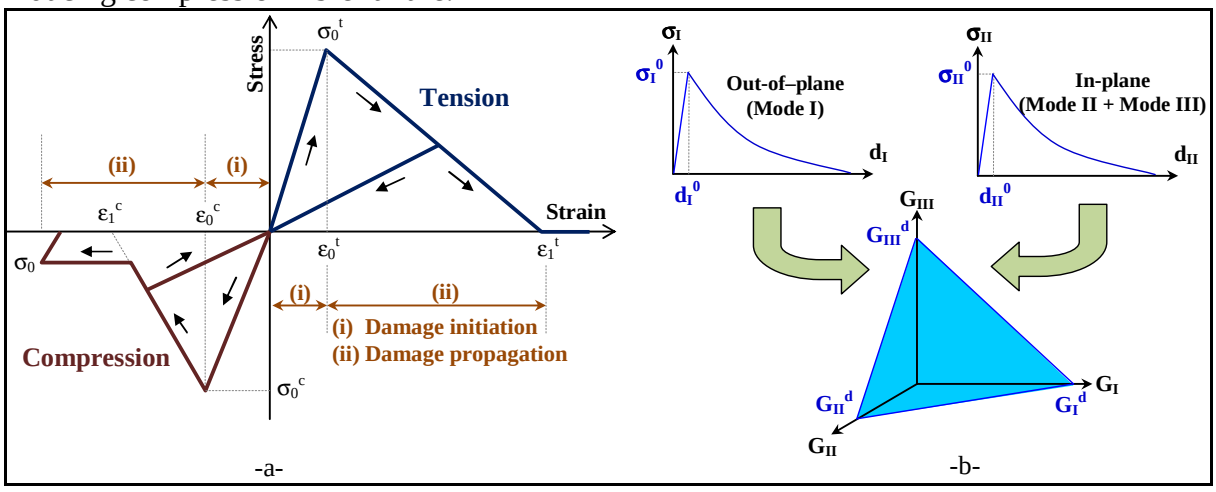


**Figure 3** Behaviour law of (a) fibre failure in longitudinal direction;
(b) Delamination in mode I and linear coupling fracture in 3 modes

### *3.2 Modelling of matrix cracking*

A particular meshing of matrix cracking, in-between neighbouring volumic elements, is introduced to non-thickness 3D cohesive elements (interface elements) in the fibre direction

(fig 2). Quadratic classic criterion of matrix cracking was then applied in these volumic elements. As soon as this criterion is reached either in one or both neighbouring volumic elements, transverse stress in cohesive elements has to be lost and its stiffness is turned to zero, meaning that the matrix is broken. Then for this damage type, the material parameters (table 1) are the matrix transverse failure $\sigma_t^f$ and the shear failure stress $\tau_{lt}^f$. The use of interface elements to take into account the matrix cracking allows to respect the discontinuous character of this damage and to obtain, without additional parameter, the coupling between this damage and the interlaminar damage, i.e. delaminations. The proof of the relevance of this modelling type has yet been showed in the literature [13].
These matrix cracks interface elements are also used to simulate the permanent indentation. Indeed the permanent indentation seems to be, with important proportion, due to blocking system of impact debris [14] and this phenomenon was taken into account in the proposed model. To do this, a "like-plasticity" model [15] was introduced in the matrix cracking interfaces in order to limit their closure after failure in tension ($\sigma_t$) and in out of plane shear ($\tau_{tz}$) directions. Consequently, two additional material parameters, $\varepsilon_t^0$ the dimensionless size of debris and $k_t$ their stiffness, are necessary to take into account the phenomenon of permanent indentation. These 2 parameters are difficult to associate to classical material parameters evaluated on classical tests and in fact are directly evaluated thanks to a reference impact test. Then this evaluation process limits the predictive character of this model, and in particular for the part linked to permanent indentation. Other works are currently in progress in order to evaluate these parameters with other and simpler experimental investigations.

*3.3 Modelling of delamination*

Delamination, formed between different orientation plies, is normally taken into account thanks to interface elements based on fracture mechanics (fig. 2a). Non-thickness 3D cohesive elements joint lower and upper volumic ply elements. The initiation of delamination is based on quadratic criterion, similar to this one of matrix cracking and its propagation on a linear coupling in 3 modes (fig. 3b). The mode I (opening) is in the thickness direction normal to delamination plane, while mode II and mode III are assumed to be equal, in the in-plane directions. Two additional material parameters are then needed, the critical energy release rate for delamination propagation in mode I $G_I^d$ and in mode II $G_{II}^d$.

| $E_l^t$ (GPa) | $E_l^c$ (GPa) | $E_t$ (GPa) | $\nu_{lt}$ | $G_{lt}$ (GPa) | $\sigma_t^f$ (MPa) | $\tau_{lt}^f$ (MPa) | $G_I^d$ (N/mm) | $G_{II}^d$ (N/mm) |
|---|---|---|---|---|---|---|---|---|
| 130 | 100 | 7.7 | 0.3 | 4.8 | 60 | 110 | 0.5 | 1.6 |

| $\varepsilon_l^t$ | $\varepsilon_l^c$ | $G_l^t$ (N/mm) | $G_l^c$ (N/mm) | $\sigma_0$ (MPa) | $\varepsilon_t^0$ | $k_t$ (MPa/mm) |
|---|---|---|---|---|---|---|
| 0.016 | -0.0125 | 133 | 10 | -200 | 0.02 | 10000 |

**Table 1** Material properties of T700/M21 for numerical simulation

## 4. Experimental validation of modelling

The composite plates were tested experimentally and numerically, at 1.6, 6.5, 17, 26.5 and 29.5 J of impact energy and the corresponding CAI tests were performed. The simulation is performed in three steps (fig. 4). The first step corresponds to the impact test, this step duration is about 5 ms. After this step, the impact damage is obtained and in particular the permanent indentation. The second step consists in the stabilization of oscillations due to impact and the modification of the boundary conditions to set up the CAI's ones. Finally the third step consists in the CAI step and the final fracture of the plate. The total calculation time

of this model is approximately 12 hours with 8 CPUs without optimization of the modelling to decrease this time.

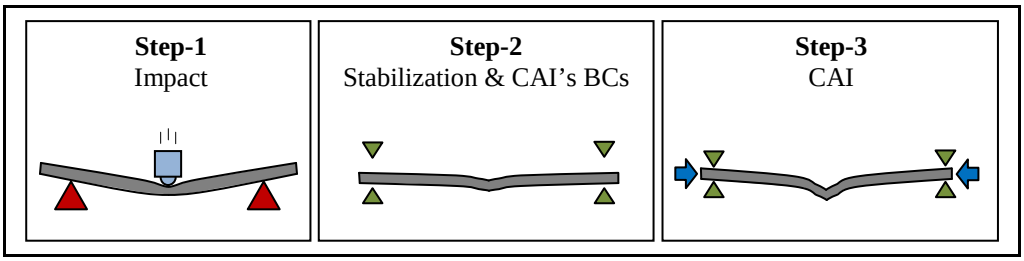


**Figure 4** The three steps of the simulation: Impact test (a); Stabilization of the plate and CAI's boundary conditions (b); and CAI test (c)

*4.1 Numerical and experimental comparison of impact test*

The comparison between the delamination areas and the force-displacement curves, obtained numerically and experimentally, are shown in figure 5. It should be noted in this figure that the 1.6 J test is not represented because no delamination, nor experimentally nor numerically, is observed. Moreover an experimental problem did not allow to obtain the 17 J curve. A relatively good correlation is observed between modelling and experiments, in particular the shape of the delaminated interfaces are well simulated, even if the area of the first interface, non impacted side, is overestimated for the highest energies. The simulated force-displacement curves take into account the different stiffness decreases: the first one at about 2 mm-displacement is soft and mainly due to delaminations, and the second one, at about 5 mm-displacement is strong and mainly due to fibre failure.

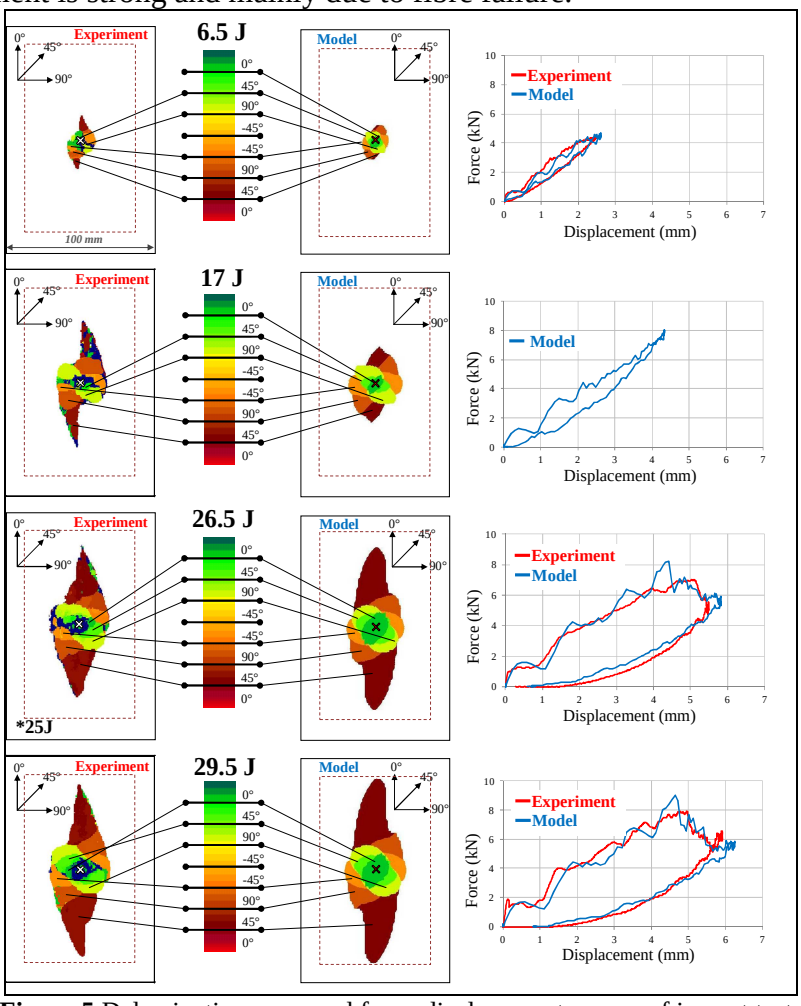


**Figure 5** Delamination areas and force-displacement curves of impact tests

These fibre failures can be observed after 29.5 J-impact in the central zone under the impactor (fig. 6). It can be noticed in this figure that only the half-plate is drawn and that the deformed shape is free of exterior loads and due to the "like-plasticity" model in the matrix cracking elements above mentioned. These fibre failures are mainly due to tension failures and only the zone just under the impactor, impacted side, presents compression failure. Moreover a fibre failure crack in compression is observed impacted side right next to the impact point (fig. 6). This crack concerns only with the first 0° ply, impacted side. Of course due to the symmetry of the modelling, this crack exists "virtually" on the other half-plate. This crack reveals to be of first importance during CAI, because its propagation induces the final fracture of the plate. In fact, this crack is not so obvious on the experiments: a little crack can be observed right next to the impact mark but its length is only a few millimetres and its orientation is not in the 90° direction but more circular. Then this crack is overestimated by the modelling, and the criterion of compression fibre failure should be improved to better take into account this damage.

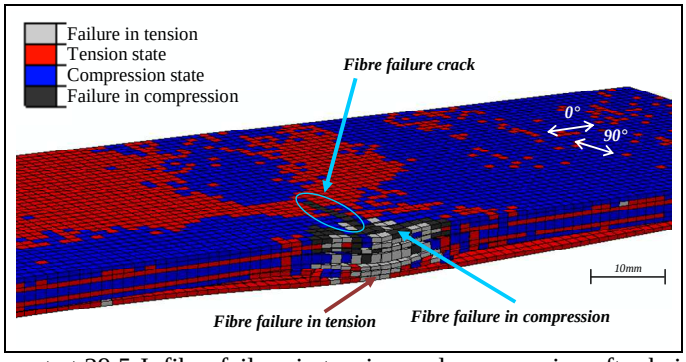


**Figure 6** Impact at 29.5 J: fibre failure in tension and compression after being impacted

*4.2 Numerical and experimental comparison of CAI test*

The comparison between the experimental and numerical CAI tests after a 29.5 J impact is shown figure 7. The stress-displacement curve (fig. 7a) corresponds to the curve of the mean stress, evaluated by dividing the load force by the section, function of the longitudinal displacement, in the 0° direction, imposed during CAI test. For the stress-deflection curve (fig. 7b), the deflection corresponds to the out-of plane displacement of the plate centre due to buckling. The fields of longitudinal strain, where the experimental field is obtained thanks to CCD cameras and image correlation, are also drawn in this figure (fig. 7c) for different loads. The strain scale is chosen to obtain red colour for positive or null strain and purple colour for strains which are less or equal than compression failure strain of T700/M21 ($\varepsilon_o^c = -0.0125$).

The stress-displacement curve (fig. 7a) shows that, until experimental failure, the modelling well simulates the experiment, however after this point, the final failure numerically obtained is not sharp enough. Nevertheless the ultimate stress is well predicted because the additional stress during failure propagation is very weak. This final failure propagation, numerically obtained, is due to the propagation of the compression failure crack above mentioned. This propagation is observed on the strain fields numerically obtained (fig. 7c). This propagation is also seen on the strain fields experimentally obtained, even if this propagation seems faster (between about -120 and -149 MPa). Moreover the crack does not seem present before -120 MPa, contrary to the modelling, but in fact it is not possible to observe it because the image inter-correlation takes as reference image the deformed shape after impact. Then the experimental strain field, obtained by image correlation, is artificially considered null after impact, which is not the case for modelling. Therefore the comparison between these two strain fields should be taken with caution.

The stress-deflection curve shows the classical phenomenon of impact damage buckling during CAI test. This phenomenon is partially simulated by modelling even if it is overestimated.

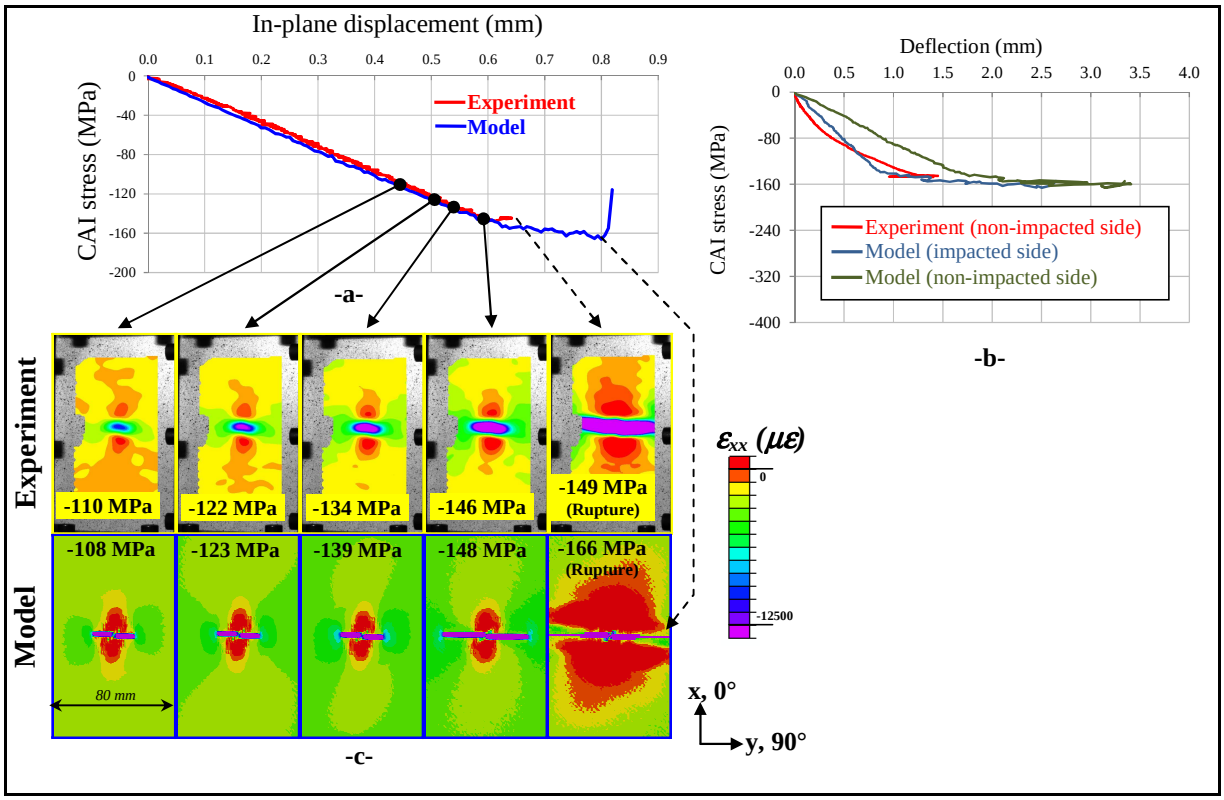


**Figure 7** CAI at 29.5 J: stress-displacement (a) and stress-deflection curves (b); longitudinal strain fields (c)

Afterwards the evolution of the CAI strength versus impact energy and indentation are drawn (fig. 8). Globally the tendencies of the impact energy influence are simulated but some improvements are yet necessary. For example, the CAI strength of the 1.6 J impact is overestimated. In fact, this impact induces no delamination and almost no damage, and then the plate failure is due to buckling or pure compression. The buckling strength of this plate simply supported on 4 edges is about 300 MPa and the compression failure strength is about 500 MPa. The experiment shows effectively a failure at about 300 MPa, due to buckling, but the model overestimates this value, due probably to stronger boundary conditions compared to experiment.

The CAI strength of the 6.5 J impact is underestimated. This should be due to overestimation of the impact damage by modelling, as for example the compression failure crack, right next to the impact point.

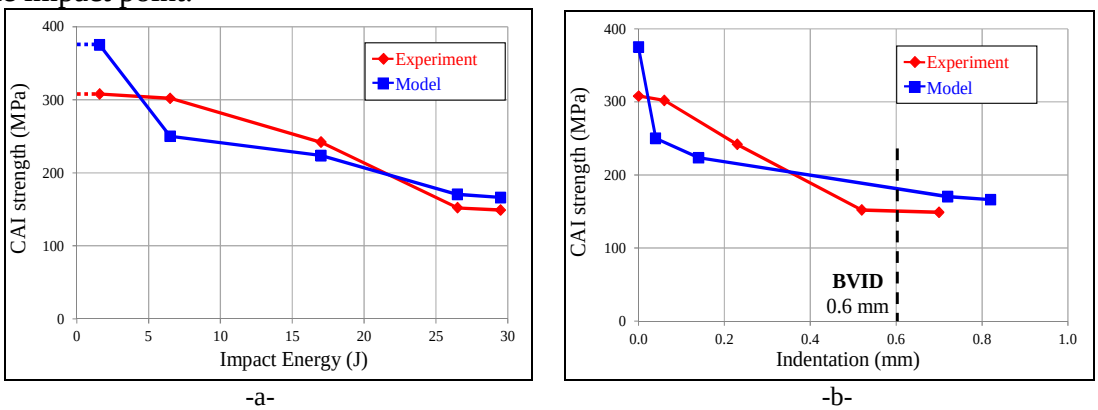


**Figure 8** CAI strength versus impact energy (a) and indentation (b) numerically and experimentally obtained

## 5. Conclusion

A model enabling to simulate the impact and CAI tests on composite laminated plates has been elaborated. It allows to globally simulate impact damages, as delaminated area, fibres failure or permanent indentation, and the CAI damages, as fibres failure propagation or local buckling of delaminated zone. It allowed to highlight the failure scenario during CAI test and to confirm the concurrence of two phenomena; the well known buckling of the impact damaged zone, and the propagation of a crack right next to the impact point. This crack, situated on impacted side, is a compression fibre failure crack created during impact which propagates under compression stress during CAI. These two phenomena develop together during CAI and induce final failure of the plate.

Finally, this modelling allows to numerically estimate the permanent indentation after impact and the residual strength and could allow to numerically optimize this plate with impact damage tolerance.

## References

[1] Abrate, S., "Impact on composites structures", Cambridge univ. press, (1998)

[2] Razi H., Ward S., "Principle for achieving damage tolerant primary composite aircraft structures", 11th DoD/FAA/NASA conf. on fibrous composites in structural design., Fort Worth, USA, (1996)

[3] Rouchon J., "Fatigue and damage tolerance aspects for composite aircraft structures", Delft, (1995)

[4] Alderliesten R.C., "Damage tolerance of bonded aircraft structures", Int. Jour. of Fati., 31, 6, pp. 1024-30 (2008)

[5] Petit S., Bouvet C., Bergerot A., Barrau J.J., "Impact and compression after impact experimental study of a composite laminate with a cork thermal shield", Comp. Sci. and Tech., 67, pp. 3286-99 (2007)

[6] Zheng D., Binienda W.K., "Effect of permanent indentation on the delamination threshold for small mass impact on plates", Int. Jour. of Sol. and Struct., 44, 25-26, pp. 8143-58 (2007)

[7] Allix O., Blanchard L., Mesomodeling of delamination: towards industrial applications, *Comp. Sci. Tech.*, 66, pp. 731-44 (2006)

[8] Choi H.Y., Chang K., A model for predicting damage in graphite / epoxy laminated composites resulting from low-velocity point impact, *Jour. Of Comp. Mat.*, 26, pp. 2134-69 (1992)

[9] Faggiani A., Falzon B.G., Predicting low-velocity impact damage on a stiffened composite panel, *Comp. Part A*, 41, 6, pp. 737–49 (2010)

[10] Bouvet C., Castanié B., Bizeul M., Barrau J.-J., Low velocity impact modelling in laminate composite panels with discrete interface elements, *Int. Jour. Sol. Struc.*, 46, pp. 2809-2821 (2009)

[11] Airbus Industries Test Method : AITM 1-0010 : Determination of compression strength after impact

[12] Pinho S.T., Robinson P., Iannucci L., Fracture toughness of the tensile and compressive fibre failure modes in laminated composites, *Comp. Sci. Tech.*, **66**, pp. 2069-2079 (2006)

[13] Wisnom M.R., Modelling discrete failures in composites with interface elements, *Comp. Part A: App. Sci. and Manuf.*, 41, 7, pp. 795-805 (2010)

[14] Abi Abdallah E., Bouvet C., Rivallant S., Broll B., Barrau J.J., Experimental analysis of damage creation and permanent indentation on highly oriented plates, *Compos. Sci. Tech.*, 69, 7-8, pp. 1238-45 (2009)

[15] Bouvet C., Rivallant S., Barrau J.J., Low velocity impact modelling in laminate composites and permanent indentation, *workshop ICA-ONR « dynamic failure of composite and sandwich structure »*, Toulouse (France), 23-24 juin (2011)